

Understanding Noise and Interference Regimes in 5G Millimeter-Wave Cellular Networks

Mattia Rebato[†], Marco Mezzavilla^{*}, Sundeep Rangan^{*}, Federico Boccardi[◇], Michele Zorzi[†]

^{*} NYU WIRELESS, Brooklyn, NY, USA

[†] University of Padova, Italy

emails: {rebatoma, zorzi}@dei.unipd.it, {mezzavilla, srangan}@nyu.edu, federico.boccardi@ieee.org

Abstract—With the severe spectrum shortage in conventional cellular bands, millimeter-wave (mmWave) frequencies have been attracting growing attention for next-generation micro- and pico-cellular wireless networks. A fundamental and open question is whether mmWave cellular networks are likely to be noise- or interference-limited. Identifying in which regime a network is operating is critical for the design of MAC and physical-layer procedures and to provide insights on how transmissions across cells should be coordinated to cope with interference. This work uses the latest measurement-based statistical channel models to accurately assess the Interference-to-Noise Ratio (INR) in a wide range of deployment scenarios. In addition to cell density, we also study antenna array size and antenna patterns, whose effects are critical in the mmWave regime. The channel models also account for blockage, line-of-sight and non-line-of-sight regimes as well as local scattering, that significantly affect the level of spatial isolation.

Index Terms—5G, millimeter wave communication, cellular systems, interference regime, noise regime

I. INTRODUCTION

The millimeter-wave (mmWave) spectrum, roughly defined as the frequencies between 10 and 300 GHz, is a new and promising frontier for cellular wireless communications [1], [2]. With the rapidly growing demand for cellular data, conventional frequencies below 3 GHz are now highly congested. For example, in the most recent FCC auction, 65 MHz of AWS-3 spectrum were sold for a record breaking \$45 billion, which shows the severe spectrum crunch encountered when trying to expand wireless networks today. In contrast, the mmWave bands offer vast and largely untapped spectrum, up to 200 times all current cellular allocations by some estimates. Due to this enormous potential, mmWave networks have been widely cited as one of the most promising technologies for Beyond 4G and 5G cellular evolution.

A fundamental and outstanding question for the design of these networks is to understand the effects of interference and, more specifically, under which circumstances mmWave cellular networks are likely to be limited by interference or by thermal noise. Identifying in which regimes networks operate is central to system design: for example, while interference limited networks can benefit from advanced techniques such as inter-cellular interference coordination, coordinated beamforming and dynamic orthogonalization, these techniques

have little value in networks where thermal noise, rather than interference, is dominant.

While for traditional (in particular macrocell-based) cellular deployments the relative power of interference to thermal noise is a function of the distance between cells and of the transmit power spectral density, the results in this paper will demonstrate that in mmWave systems the relative strength of interference depends on many more factors. Most importantly, mmWave systems rely on highly directional transmissions to overcome the high isotropic path loss. Directional transmissions tend to isolate users, thereby reducing the interference. However, the degree of isolation depends strongly on the size of the antenna arrays, the antenna pattern, and the level of local scattering and spatial multipath. In addition, mmWave signals can be blocked by many common materials, eliminating long distance links. This potentially improves the isolation but may also lead to coverage holes. There are also significant differences in path loss for mobiles in Line-of-Sight (LoS) and Non-Line-of-Sight (NLoS) locations.

The broad purpose of this paper is to leverage detailed measurement-based statistical channel models to provide an accurate assessment of the Interference-to-Noise Ratio (INR), and of its relation to various key deployment parameters including base station density, transmit power, bandwidth and antenna pattern. Our analysis uses the latest channel models for 28 and 73 GHz based on extensive New York City measurements [2]–[5].

The rest of the paper is organized as follows. In Section II we present the prior art related to interference and noise evaluations. In Section III we describe the scenarios simulated. A preliminary numerical evaluation, along with some important remarks, is reported in Section IV. Finally, we conclude the paper and describe some future research steps in Section V.

II. RELATED WORK

In [6] and [7], the authors outline the challenges of interference management in 5G cellular networks, overviewing techniques such as Coordinated MultiPoint (CoMP) and other advanced interference management techniques.

In [8], a new mathematical framework for the analysis of mmWave cellular networks is presented. The paper introduces a multi-ball approximation that lies in replacing the LoS or NLoS probability of typical User Equipment (UE) with an approximate function, which still depends on the Base Station (BS) to UE distance d but is piece-wise constant as a function

[◇] F. Boccardi's work was carried out in his personal capacity and the views expressed here are his own and do not reflect those of his employer (Ofcom).

of d . A noise-limited approximation is found to be quite accurate for a small density of BSs. However, when the density of BSs increases, thus decreasing the average cell radius, the approximation no longer holds.

Noise-limited and interference-limited regimes are studied for ad hoc mmWave networks at 60 GHz operating under slotted ALOHA and Time Division Multiple Access (TDMA) protocols in [9] and [10]. These works consider networks at 60 GHz, motivated by the fact that a lot of research has been done in the last years to support the development of WiGig [11]. However, we note that propagation at 60 GHz is heavily affected by the peak of oxygen absorption, and for this reason different Access Points (APs) will be more isolated than at 28 or 73 GHz. Different scenarios are studied and implemented from both analytical and simulation standpoints. As a result, [9] and [10] suggest the use of a hybrid MAC protocol that works in two distinct phases; a distributed contention-based resource allocation, which is more suitable for the noise-limited regime, followed by a centralized contention-free resource allocation, which is more suitable for the interference-limited regime.

In [12], an analytical framework is proposed to evaluate the instantaneous INR distribution of an outdoor mmWave ad hoc network working at 60 GHz. The authors consider a narrowband channel model with transmitter locations forming a Poisson Point Process (PPP), and capture mmWave features by considering directional beamforming and LoS/NLoS configurations. It is shown that, in a very dense network (e.g., 1000 sources/km²), the interference power is nearly always higher than the noise power. This motivates novel ad hoc mmWave architectures to deal with interference in order to realize networks that can achieve gigabit speeds.

Some general results related to interference and noise regimes for mmWave cellular networks have been presented in [13] and [14], which motivated us to run a more detailed campaign of simulations at varying operating configurations. The work in [15] used simple approximations of the channel propagation to identify scaling laws for the bandwidth, number of antennas and transmit power under which the network would be in an interference or noise-limited regime.

Reference [16] studies the feasibility of spectrum pooling in mmWave cellular networks under ideal conditions at both 28 and 73 GHz, and [17] studies the impact of coordination between different networks, under the assumption of ideal beamforming. In both [16] and [17], beamforming is modeled as an ON/OFF beam.

Our INR evaluation introduces some key additional contributions: (i) a detailed *lobe*-shaped antenna pattern to precisely capture the mmWave beamforming gains¹; (ii) an updated channel model at both 28 and 73 GHz², which, together with a more realistic beamforming model, provides a very accurate characterization of the useful and interfering received signal;

and (iii) a comparison of a blind allocation vs. a centralized upper bound vs. an interference-less case. We believe that these additional contributions, with respect to the previous work, are an important step forward towards a more realistic understanding of the role of interference in 5G mmWave system design.

III. SYSTEM MODEL

We consider a mobile network where BSs and UEs are deployed following a PPP with density λ_{BS} and λ_{UE} , respectively. Moreover, the use of this unplanned deployment where the BS positions are not optimized is suitable to model the case where APs are deployed by users in a similar way to WiFi today. Our simulations follow a Monte Carlo approach, in which many independent experiments³ are repeated to empirically derive statistical quantities of interest. Without loss of generality, we evaluate the performance of a typical receiver located in the origin of the area considered, whose statistics are estimated based on 50000 repetitions of this procedure.

Thanks to a detailed channel and antenna characterization, we can compute the Signal-to-Interference-plus-Noise-Ratio (SINR) between transmitter i and receiver j as:

$$\text{SINR}_{ij} = \frac{\frac{P_{Tx}}{PL_{ij}} G_{ij}}{\sum_{k \neq i} \frac{P_{Tx}}{PL_{kj}} G_{kj} + BW \times N_0}, \quad (1)$$

where k represents each interfering link, BW is the total bandwidth, N_0 is the thermal noise, P_{Tx} is the transmitted power, G is the beamforming gain, and PL is the pathloss between the receiver UE and the associated BS.

The pathloss is modeled with three states, as reported in [19]: LoS, NLoS and outage as a function of the distance d between transmitter and receiver. In the simulations, UEs are associated to the BS that provides the smallest pathloss. The channel is modeled as reported in [19], which represents a dense urban environment. A precise *lobe*-shaped beamforming gain G is computed by multiplying the Multiple-Input and Multiple-Output (MIMO) beamforming vectors⁴ by the channel matrix. The beamforming gain from transmitter i to receiver j is given by:

$$G_{ij} = |\mathbf{w}_{R_{x_{ij}}}^* \mathbf{H}_{ij} \mathbf{w}_{T_{x_{ij}}}|^2, \quad (2)$$

where $\mathbf{w}_{T_{x_{ij}}} \in \mathbb{C}^{n_{Tx}}$ is the beamforming vector of transmitter i when transmitting to receiver j , $\mathbf{w}_{R_{x_{ij}}} \in \mathbb{C}^{n_{Rx}}$ is the beamforming vector of receiver j when receiving from transmitter i , and \mathbf{H} is the channel matrix. Both vectors are complex, with length equal to the number of antenna elements in the array. The use of beamforming is essential in mmWave communications, as the gain obtained from directional beam steering is a critical factor to achieve a sufficient link margin. We assume to have the possibility of steering in any direction, i.e., we can generate a beamforming vector for any possible

¹A precise description of the model used in this paper can be found in [18].

²We use the NYU channel models for 28 GHz and 73 GHz frequencies [19] based on measurement campaigns carried out in a real dense urban environment, as reported in [2]–[5].

³More precisely, experiments are independent because the deployment of the devices in the area is randomly generated at each iteration.

⁴The beamforming vectors are computed as reported in [20]. This antenna gain model is detailed and complete with main and side-lobes.

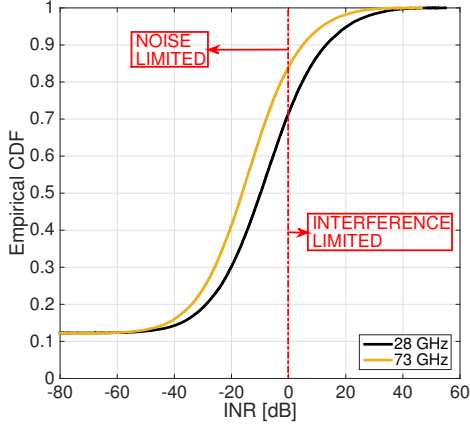


Figure 1: Empirical CDF of the INR for $\lambda_{UE} = 300$ UEs/km² and $\lambda_{BS} = 30$ BSs/km².

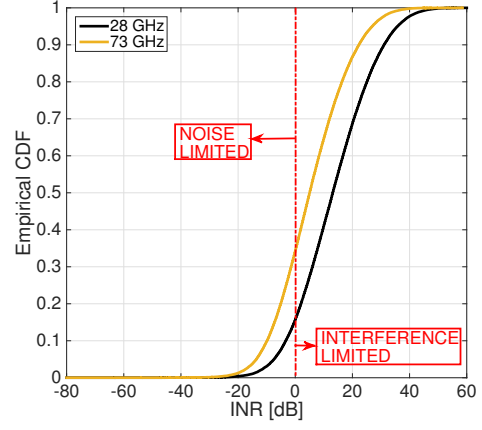


Figure 3: Empirical CDF of the INR for $\lambda_{UE} = 900$ UEs/km² and $\lambda_{BS} = 90$ BSs/km².

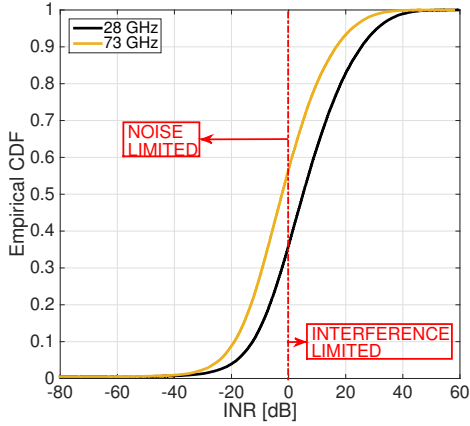


Figure 2: Empirical CDF of the INR for $\lambda_{UE} = 600$ UEs/km² and $\lambda_{BS} = 60$ BSs/km².

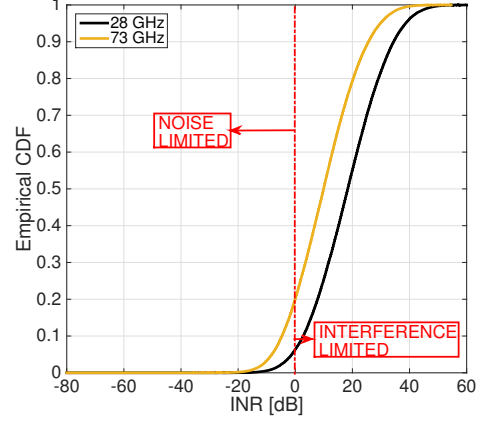


Figure 4: Empirical CDF of the INR for $\lambda_{UE} = 1200$ UEs/km² and $\lambda_{BS} = 120$ BSs/km².

angle between 0 and 360 degrees. With this transmission, the two beams (i.e., the one of the UE and the one of the BS) are always perfectly aligned. From a realistic point of view, the set of beampatterns is discrete, and performing the steering in an arbitrary direction may be too costly or even impossible.

IV. SIMULATION RESULTS

We consider a 64 elements (8×8) Uniform Planar Array (UPA) antenna at the BS, while at the receiver side we have a UPA with 16 elements (4×4).

For the analysis in this paper, we focus on the INR, which is defined as:

$$\text{INR}_{ij} = \frac{\sum_{k \neq i} \frac{P_{Tx}}{PL_{kj}} G_{kj}}{BW \times N_0}, \quad (3)$$

where at the numerator we sum all the interfering links by multiplying their transmit powers P_{Tx} , beamforming gains G and respective pathloss values PL . The denominator comprises the thermal noise power, which is equal to the power spectral density N_0 multiplied by the total bandwidth BW .

We report, for each case, the Empirical Cumulative Distribution Function (ECDF) of the downlink INR defined in (3), and identify $\text{INR} = 0$ dB as the transitional point that determines the shift from a noise-limited to an interference-limited regime.

In our simulation campaign, we have considered a 7 dB Noise Figure (NF), a 500 MHz total bandwidth, and a transmit power $P_{Tx} = 30$ dBm, which are in line with the specifications envisioned for future 5G mmWave mobile networks considering a downlink transmission.

By observing Figures 1 – 4, we can derive the following general insights.

1) *Higher BSs density, higher interference:* A first (obvious) result is that interference increases with the number of base stations, therefore increasingly biasing towards the interference limited regime. We show that we start observing the majority of links ($> 80\%$) operating in the interference limited region for $\lambda_{BS} = 120$ BSs/km².

It is important to note that a large amount of interference is generated from the symmetric lobe. We reserve as a future work the study of a scenario where an antenna model that blocks symmetric lobes is applied. We have also verified that

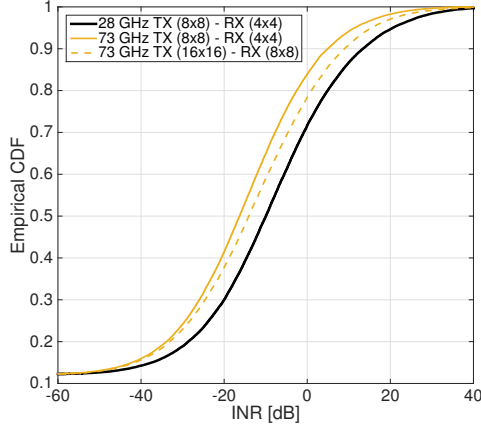


Figure 5: Empirical CDF of the INR for $\lambda_{BS} = 30$ BSs/km² and $\lambda_{UE} = 300$ BSs/km².

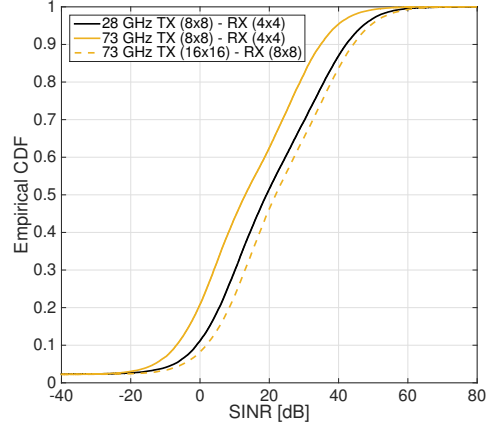


Figure 6: Empirical CDF of the SINR for $\lambda_{BS} = 30$ BSs/km² and $\lambda_{UE} = 300$ BSs/km².

changes in the density of the UEs λ_{UE} for fixed λ_{BS} do not affect the behavior of the INR curves. In fact, as long as the number of active BSs (and so the active number of interfering source) remains the same, the behavior of the INR does not change. However, we note that this holds under the assumption of full-buffer UEs.

2) *Higher band, lower interference:* At 73 GHz, due to a higher pathloss, interference is ~ 10 dB less than the interference experienced at lower mmWave bands (28 GHz). Please note that in these first simulations we consider the same number of antennas for both frequencies. Nonetheless, at higher operating bands we could deploy more antennas in the same area, which would result in higher directionality, and therefore even less interference.

3) *Interferers domains:* We report in Table I the distributions of interfering link states for the 28 GHz curve of Figure 1. The table reports the probability for an interferer to be in one of the three states (LoS, NLoS, and outage) for the two ECDF intervals. We split the curve into two intervals in order to capture the relation between the state of the interferers and the INR value.

ECDF interval	LoS	NLoS	outage
[0% - 12%]	0%	0%	100%
[12% - 100%]	1%	18%	81%

Table I: Empirical probabilities to be in LoS, NLoS or outage for the interferers of Figure 1 (the case in which $\lambda_{UE} = 300$ UEs/km² and $\lambda_{BS} = 30$ BSs/km²). We provide the statistics for two ECDF intervals (0 - 12% and 12 - 100%), that represent different trends in the plot of Figure 1.

It is interesting to note how, for low BS density scenarios, the dominant interfering links are in outage, thus obviously reflecting a noise-limited regime. As observed, at higher BS densities, the states of the interferers become NLoS and LoS, thus increasingly biasing the system towards interference limited regimes.

These results allowed us to identify three main working regimes.

- When the BS density is smaller than 30 BSs/km² (average cell radius bigger than 103 m), the mmWave cellular network can be assumed to be **noise-limited**. In such a regime, interference coordination will not be necessary.
- Conversely, when the density is above 120 BSs/km², the mmWave cellular network can be assumed to be **interference-limited**. Under this assumption, some sort of interference coordination is needed.
- Finally, we captured an intermediate case, where the density is between 30 and 120 BSs/km²; here, we can observe both regimes. For this particular state, any user can be either **noise-limited** or **interference-limited**. We may need a hybrid coordination scheme in this case.

4) *More antenna elements at 73 GHz:* So far, we have considered the same antenna array size for both frequencies. Nonetheless, because of the reduced wavelength at 73 GHz, we can deploy a higher number of antenna elements in the same area.

Figures 5 and 6 report the INR and the SINR ECDFs, respectively. The two cases considered before (solid lines, same number of antennas) are compared to a configuration with an increased number of antennas at 73 GHz, i.e., 16×16 at the transmitter and 8×8 at the receiver (dashed line). The results show that using more antennas results in a slightly increased interference (about 2–3 dB in most cases, see Figure 5). While the average interference due to the main transmit/receive lobes is expected to be roughly the same in the two cases (as the increased gain is compensated by the correspondingly reduced beamwidth), with more antennas the effect of the side lobes is larger, and the interference variance is also larger, thus resulting in an increased INR. On the other hand, the higher directivity of the larger arrays (which in this specific example provides a total gain of 12 dB, i.e., a factor of 4 at both sides) results in an increased SINR value (about 9–10 dB, see Figure 6).

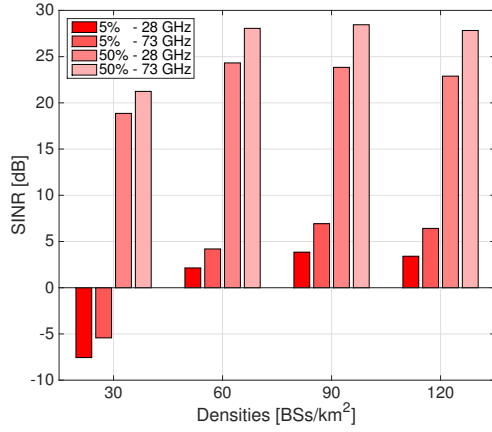


Figure 7: Performance comparison at increasing BS densities for both 28 GHz and 73 GHz.

Finally, we report in Figure 7 the 5th and 50th percentiles of the SINR at 28 GHz and 73 GHz vs. the BS density. An improvement of the SINR when the BS density is increased corresponds to a noise-limited regime, whereas in an interference-limited regime densification leads to a similar increase of both the intended signal and the interference, making the SINR weakly dependent on the BS density (this change of regime occurs between 60 and 90 BSs/km² for the 5th percentile, and between 30 and 60 BSs/km² for the 50th percentile). Note that the slight SINR decrease when the BS density is further increased is due to the fact that some interferers move from NLoS to LoS condition, so that their power increases more than that of the intended signal (an effect more visible at 28 GHz).

V. CONCLUSION

This paper leverages the latest measurement-based channel models to accurately assess the interference statistics in a wide range of deployment scenarios. The channel models also account for blockage, line-of-sight and non-line-of-sight regimes, as well as local scattering, that significantly affect the level of spatial isolation.

Determining the regime in which the network is operating, and specifically whether it is noise- or interference-limited, is critical in order to properly design MAC and physical-layer procedures. In this paper, we capture each operating regime as a function of the transmitter density at two different frequencies, i.e., 28 GHz and 73 GHz, and observe their different trends, which depend on directionality and propagation characteristics.

Based on our findings, we believe that a flexible, user-centric, interference-aware MAC protocol may represent the right solution to better leverage the mmWave potential, which motivates us to further investigate these possibilities as part of our future work.

REFERENCES

- [1] T. S. Rappaport, R. W. Heath Jr., R. C. Daniels, and J. N. Murdock, *Millimeter Wave Wireless Communications*. Pearson Education, 2014.
- [2] T. S. Rappaport, S. Sun, R. Mayzus, H. Zhao, Y. Azar, K. Wang, G. N. Wong, J. K. Schulz, M. Samimi, and F. Gutierrez, "Millimeter Wave Mobile Communications for 5G Cellular: It Will Work!" *IEEE Access*, vol. 1, pp. 335–349, 2013.
- [3] Y. Azar, G. Wong, K. Wang, R. Mayzus, J. Schulz, H. Zhao, F. Gutierrez, D. Hwang, and T. Rappaport, "28 GHz Propagation Measurements for Outdoor Cellular Communications Using Steerable Beam Antennas in New York City," in *IEEE International Conference on Communications (ICC)*, June 2013, pp. 5143–5147.
- [4] H. Zhao, R. Mayzus, S. Sun, M. Samimi, J. Schulz, Y. Azar, K. Wang, G. Wong, F. Gutierrez, and T. Rappaport, "28 GHz Millimeter Wave Cellular Communication Measurements for Reflection and Penetration Loss in and Around Buildings in New York City," in *IEEE International Conference on Communications (ICC)*, June 2013, pp. 5163–5167.
- [5] M. Samimi, K. Wang, Y. Azar, G. Wong, R. Mayzus, H. Zhao, J. Schulz, S. Sun, F. Gutierrez, and T. Rappaport, "28 GHz Angle of Arrival and Angle of Departure Analysis for Outdoor Cellular Communications Using Steerable Beam Antennas in New York City," in *IEEE 77th Vehicular Technology Conference (VTC Spring)*, June 2013, pp. 1–6.
- [6] W. Nam, D. Bai, J. Lee, and I. Kang, "Advanced Interference Management for 5G Cellular Networks," *IEEE Communications Magazine*, vol. 52, no. 5, pp. 52–60, May 2014.
- [7] E. Hossain, M. Rasti, H. Tabassum, and A. Abdelnasser, "Evolution Toward 5G Multi-Tier Cellular Wireless Networks: An Interference Management Perspective," *IEEE Wireless Communications*, vol. 21, no. 3, pp. 118–127, June 2014.
- [8] M. Di Renzo, "Stochastic Geometry Modeling and Analysis of Multi-Tier Millimeter Wave Cellular Networks," *IEEE Transactions on Wireless Communications*, vol. 14, no. 9, pp. 5038–5057, Sept 2015.
- [9] H. Shokri-Ghadikolaei and C. Fischione, "The Transitional Behavior of Interference in Millimeter Wave Networks and Its Impact on Medium Access Control," *IEEE Transactions on Communications*, vol. 64, no. 2, pp. 723–740, Feb 2016.
- [10] H. S. Ghadikolaei and C. Fischione, "Millimeter Wave Ad Hoc Networks: Noise-limited or Interference-limited," *CoRR*, vol. abs/1509.04172, 2015. [Online]. Available: <http://arxiv.org/abs/1509.04172>
- [11] Wireless Gigabit (WiGig) Alliance, "WiGig White Paper: Defining the Future of Multi-Gigabit Wireless Communication," Tech. Rep., 2010.
- [12] A. Thornburg, T. Bai, and R. Heath, "Interference Statistics in a Random MmWave Ad Hoc Network," in *IEEE International Conference on Acoustics, Speech and Signal Processing (ICASSP)*, April 2015, pp. 2904–2908.
- [13] S. Rangan, T. Rappaport, and E. Erkip, "Millimeter-Wave Cellular Wireless Networks: Potentials and Challenges," *Proceedings of the IEEE*, vol. 102, no. 3, pp. 366–385, March 2014.
- [14] T. Bai and R. Heath, "Coverage and Rate Analysis for Millimeter-Wave Cellular Networks," *IEEE Transactions on Wireless Communications*, vol. 14, no. 2, pp. 1100–1114, Feb 2015.
- [15] F. Gomez-Cuba, S. Rangan, and E. Erkip, "Scaling Laws for Infrastructure Single and Multihop Wireless Networks in Wideband Regimes," in *IEEE International Symposium on Information Theory (ISIT)*, June 2014, pp. 76–80.
- [16] A. K. Gupta, J. G. Andrews, and R. W. Heath, "On the Feasibility of Sharing Spectrum Licenses in mmWave Cellular systems," *CoRR*, vol. abs/1512.01290, 2015. [Online]. Available: <http://arxiv.org/abs/1512.01290>
- [17] F. Boccardi, H. Shokri-Ghadikolaei, G. Fodor, E. Erkip, C. Fischione, M. Kountouris, and P. Popovski, "Spectrum Pooling in MmWave Networks: Opportunities, Challenges, and Enablers," *ArXiv e-prints*, Mar. 2016. [Online]. Available: <http://arxiv.org/abs/1603.01080>
- [18] M. Rebato, M. Mezzavilla, S. Rangan, and M. Zorzi, "Resource Sharing in 5G mmWave Cellular Networks," in *IEEE INFOCOM Millimeter-wave Networking Workshop (mmNet 2016)*, San Francisco, USA, Apr. 2016.
- [19] M. Akdeniz, Y. Liu, M. Samimi, S. Sun, S. Rangan, T. Rappaport, and E. Erkip, "Millimeter Wave Channel Modeling and Cellular Capacity Evaluation," *IEEE Journal on Selected Areas in Communications*, vol. 32, no. 6, pp. 1164–1179, June 2014.
- [20] D. Tse and P. Viswanath, *Fundamentals of Wireless Communication*. New York, NY, USA: Cambridge University Press, 2005.